
RESEARCH NOTE

NUMERICAL MODELING OF MOLD FILLING AND CURING IN NON-ISOTHERMAL RTM PROCESS

M.R. Shahnazari and A. Abbassi

*Department of Mechanical Engineering, Amirkabir University of Technology
Hafez Avenue, P.O. Box 15875-4413, Tehran, Iran, abbassi@aut.ac.ir*

(Received: June 7, 2003 – Accepted in Revised Form: October 14, 2004)

Abstract Resin Transfer Molding (RTM) is a composite manufacturing process. A preformed fiber is placed in a closed mold and a viscous resin is injected into the mold. In this paper, a model is developed to predict the flow pattern, extent of reaction and temperature change during filling and curing in a thin rectangular mold. A numerical simulation is presented to predict the free surface and its interactions with heat transfer and cure for flow of a shear-thinning resin through the preformed fiber. Finite difference method with marker and cell procedure has been used for front flow position prediction. To verify the model results, the temperature profiles for preformed fiber have been calculated, and compared with the experimental results of the other researchers. The results showed that, to optimize the better quality of production of composite materials, and also considering the effect of curing on temperature distribution during the process, the heat dispersion term should not be neglected.

Key Words Resin Transfer Molding (RTM), Porous Media, Composites Processing, Curing

چکیده آر-تی-ام یک فرآیند تولید ماده مرکب به شمار می‌رود. فیبری متخلخل درون یک قالب قرار گرفته و یک رزین ویسکوز درون آن تزریق می‌گردد. این مقاله مدلی را برای پیش‌بینی الگوی جریان، توسعه واکنش و تغییر دما در خلال فرآیند در یک قالب چهار گوش نازک ارائه می‌کند. از روش اختلاف محدود همراه با رویه مارکر و سل جهت پیش‌بینی موقعیت سطح آزاد استفاده شده است. به منظور کنترل نتایج، توزیع دما درون قالب محاسبه و با نتایج سایر محققین مقایسه شده است. نتایج نشان می‌دهند که به منظور بهینه کردن فرآیند و همچنین لحاظ کردن تاثیر واکنش فرآیند بر توزیع دما، از ضریب پخش حرارتی مکانیکی نمی‌توان صرف‌نظر کرد.

1. INTRODUCTION

The liquid molding process is of strong economical interest for the production of medium quantities of very high quality composite materials. In fact, the cost reduction of such a material is of prime importance. Therefore, it is important to restrict, as much as possible, the time needed to design the mold and the delivery system. Moreover, one should determine the optimal processing parameters. To analyze the process, a numerical simulation is one of the cheapest ways to evaluate the required injection duration at the best condition. In this forming process (RTM), a liquid resin is injected into a mold where a fiber mat has been placed

beforehand. As the result of heat activation, the filling is performed before resin solidification. Since, the fiber orientation is perfectly controlled in this method; there are some advantages of this process with respect to the conventional injection or compression molding of fiber suspension.

Heat transfer in a porous material depends on the molecular construction of medium. Therefore, during the non-isothermal RTM process, conduction and convection heat transfer play an important role [1]. A convenient numerical modeling to analyze the heat transfer is based on the volumetric averaging of field quantities.

The discrepancy between the microscopic thermal convection and the volumetric averaging

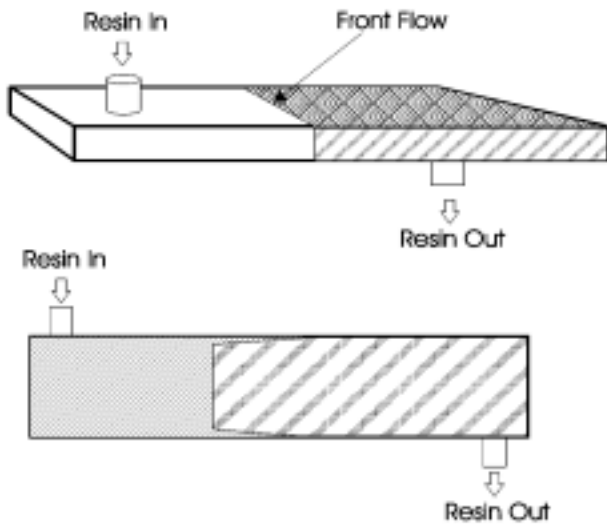


Figure 1. Schematic of problem.

is called the mechanical heat dispersion. The heat dispersion term was neglected by [2] in non-isothermal RTM process. Tucker and Dessenberger [3] showed that heat dispersion is important in typical RTM process by conducting a non-dimensional analysis. Dessenberger and Tucker [4] conducted some experiments by using random performs and compared the numerical results with and without dispersion term. Of course, they applied the local thermal equilibrium model in their study, which assumes that the fiber tows and resin system reach the same temperature instantaneously on contact. To simplify the analysis, the RTM process can be divided into mixing, filling and curing stages. A general overview of RTM modeling can be found in the review of Mal and Castro [5-7].

In the present paper, a model for the non-isothermal simulation of RTM is investigated. Also, the influence of the curing reaction on the filling is studied. The thermal behavior of the resin and the reinforcement is analyzed. Finite difference method with marker and cell procedure was applied as a numerical method to analyze the model.

2. THEORY

To consider the mathematical model, the relevant

dimension according to experimental specimen was chosen. Figure 1 shows a simple schematic of the process. The first average concept to be considered is porosity. It is defined as the local ratio of the volume to be filled by the liquid to the total volume.

$$\varepsilon_f = \frac{V_f}{V} \quad (1)$$

The average velocity vector $\langle u_f \rangle$ is called the Darcy velocity. This concept can directly provide the flow rate across any section. It differs from the intrinsic phase velocity $\langle u_f \rangle^f$, which is defined as the average velocity in the liquid phase only and provides the front flow velocity during filling. The relation links the Darcy and intrinsic phase velocities:

$$\varepsilon_f \langle u_f \rangle^f = \langle u_f \rangle \quad (2)$$

The assumptions, which were used in this model, are as follows:

- The flow is one-dimensional.
- Local thermal equilibrium exists between the liquid and solid phases.
- All the properties are constant.
- There is no consolidation and the wetting of individual fibers plays a negligible role as compared to the flow around the fiber bundles.
- Heat is transferred by convection in X-direction. Conduction heat transfer is in X and Y directions. The flow equation in X-direction is determined by Darcy equation [8]:

$$\langle u_f \rangle = -\frac{1}{\mu} K_x \nabla < P_f \rangle^f \quad (3)$$

It should be noted that other mathematical models, which include inertia term like Forschheimer model, could be used. However, in this work, due to flow velocity ranges Darcy's equation has been applied. The temperature field plays a major role in the resin transfer molding and can strongly affect the flow through its influence on the fluid viscosity. Therefore, the effects of two phases must be taken into account in each equation, which will undoubtedly increase the accuracy of the results. The local thermal equilibrium assumption is

completely valid for the process, for two reasons. Firstly, it is impossible to measure each phase temperature separately. Secondly, the characteristic time governing the heat transfer between the liquid and solid phases is small as compared with the process time scale. As a result, a single temperature for solid and fluid must be considered [8]:

$$\langle T_f \rangle^f = \langle T_s \rangle^s = \langle T \rangle \quad (4)$$

The subscript f, s in the equation refers to the, liquid phase (resin) and solid phase (fiber mat), respectively. In order to get a unique energy equation, the contributions of the liquid and solid phases must be added. Hence, the resulting equation is as follows [5]:

$$\begin{aligned} & \left((\epsilon \rho C_p)_f + (\epsilon \rho C_p)_s \right) \frac{\partial \langle T \rangle}{\partial t} + \\ & (\rho C_p)_f \langle V_f \rangle \cdot \nabla \langle T \rangle = \nabla \cdot \left((k_e + k_D) \cdot \nabla \langle T \rangle \right) + \\ & \epsilon_f \rho_f \Delta H F(T, C) \end{aligned} \quad (5)$$

where C_p denotes heat capacity, K_e is average molecular thermal diffusion tensor. Also, K_D is the mechanical mixing tensor ΔH is the reaction heat and the function $F(T, C)$ represents the curing kinetics. These two tensors can be explained as below:

$$k_e = \sum_{i=s,f} \left(\epsilon_i I + \frac{1}{V} \int_{s_i} n b_i ds \right) \quad (6)$$

$$k_D = \sum_{i=s,f} - \frac{(C_p)}{V} \int_{y_i} (u_i - \langle u \rangle) b_i dV \quad (7)$$

Where b shows the deviation vector between microscopic temperature and local equilibrium temperature which is:

$$T_i = \langle T \rangle + b_i \cdot \nabla \langle T \rangle \quad (8)$$

The boundary conditions on the wall and at inflow are Dirchlet condition, and can be written as follows:

$$\langle T \rangle = T_{wall} \quad (9)$$

and front flow velocity is:

$$U_{front} = \langle u_f \rangle^f = \frac{\langle u \rangle}{\epsilon_f} e_x \quad (10)$$

The species balance equation is written in the form as follows:

$$\begin{aligned} & \epsilon \rho_f \frac{\partial c}{\partial t} + \rho_f (\langle u_f \rangle \cdot \nabla C) = \\ & \nabla \cdot (D_d \cdot \nabla C) + \epsilon_f \rho_f F(T, C) \end{aligned} \quad (11)$$

Where it is assumed that the molecular diffusion within the macro molecular medium is negligible, while mechanical dispersion is governed by the tensor D_d .

By definition, $P_e = (\rho c_p)_f \langle u \rangle dp / 2k_f$, in which dp is the equivalent solid particle diameter. So, it is assumed $P_e \ll 1$. Therefore, the effects of k_{xx} and C_{hcx} can be neglected. Now, the energy equation can be rearranged as below:

$$\begin{aligned} \bar{T} = & - \frac{4}{\pi} \sum_{n=0}^{\infty} \frac{(-1)^n}{(2n+1)} \cos[(2n+1)\pi/2y/h] \\ & \exp\left[-(n+1/2)^2 \pi^2 \bar{x}\right] \end{aligned} \quad (12)$$

$$\bar{T} = (T - T_{inf low}) / (T_{wall} - T_{inf low}) \quad (13)$$

$$\bar{x} = k_{yy} x / (\rho c_p)_f h^2 U \quad (14)$$

At the characteristic length, x_c , the reduction in temperature has occurred in the middle of the duct. x_c , can be obtained from Equation 12. By considering $y_c = h$ and Equation 5, the conduction heat transfer term in x-direction can be neglected as follows:

$$\frac{k_{yy}}{k_{xx}} \left(\frac{x_c}{h} \right) \gg 1 \quad (15)$$

Equation 5 can be rearranged as below:

$$\begin{aligned} & ((\rho C_p)_s \epsilon_s + (\rho C_p)_f \epsilon_f) \frac{\partial \langle T \rangle}{\partial t} + \\ & (\rho c_p)_f \langle u \rangle_x \frac{\partial T}{\partial x} = \\ & \left[k_{xx} \frac{\partial^2 \langle T \rangle}{\partial x^2} + k_{yy} \frac{\partial^2 \langle T \rangle}{\partial y^2} \right] + \epsilon_f \rho_f \Delta H \\ & F(T, C) \end{aligned} \quad (16)$$

where

$$k_{xx} = k_{\text{exx}} + k_{\text{Dxx}} - \langle u \rangle_x C_{\text{hcx}} \quad (17)$$

$$k_{yy} = k_{\text{eyy}} + k_{\text{Dyy}} \quad (18)$$

By applying the scale analysis in the previous section, it can be shown that the effect of thermal diffusion cannot be neglected for the fluids with $P_e > 1$.

Effect of k_{xx} is negligible. For example, with

$$x_c = 0.52 \text{ \& } \left(\frac{x_c}{h} \right)^2 = 2704, \quad P_e = 1.4, \quad \text{the}$$

inequality $\left(\frac{k_{yy}}{k_{xx}} \right) \left(\frac{x_c}{h} \right)^2 \gg 1$ holds, because k_{xx}

has the same magnitude of k_{yy} . Therefore, the energy and species balance equations can be written as follows:

$$\begin{aligned} & ((\epsilon \rho C_p)_s + (\epsilon \rho C_p)_f) \frac{\partial \langle T \rangle}{\partial t} + (\rho C_p)_f \langle u \rangle_x \frac{\partial T}{\partial x} = \\ & (k_{yy}) \frac{\partial^2 \langle T \rangle}{\partial y^2} + \epsilon_f \rho_f \Delta H F(T, C) \end{aligned} \quad (19)$$

and

$$\begin{aligned} & \rho_f \epsilon_f \frac{\partial c}{\partial y} + \rho_f \langle u \rangle_x \cdot \langle \nabla C \rangle = \\ & D_d \frac{\partial^2 \langle c \rangle}{\partial y^2} + \epsilon_f \rho_f F(T, C) \end{aligned} \quad (20)$$

The kinetic mechanism is more complex than simple second order [7]. However, for process modeling what had to be used was the only phenomenological reaction, which is:

$$F(T, C) = K \cdot \exp\left(-\frac{E}{RT}\right) C_a^2 \quad (21)$$

3. NUMERICAL METHOD

The mid-surface of the part is covered at the outset of the simulation by a fixed mesh over which the flow front is moved. The highly non-linear character of the equations suggests a decoupled iterative solution strategy for this purpose. The simulation comprises a set of modules devoted to calculate the pressure, velocity, temperature and conversion degree fields at each time step separately.

The calculation begins at the mold entrance at each time step and proceeds upstream. The program switches from main flow to front flow. The global algorithm manages the interaction between the different modules. A simple iterative strategy was selected. From the knowledge of all fields at time t_n and an estimate of these fields at time t_{n+1} , a new estimate of these fields is obtained at time t_{n+1} . The values of velocity components over the constant displacement curvature of each cell can be related to the velocity components of each mesh using Taylor's series.

A trial and error method was applied to increase the accuracy of the results, as follows:

$$\Delta x^{\text{new}} = (u_k^{n+1} - u_k^n) \Delta t \quad (22)$$

To solve energy and species balance equations, an implicit finite difference method has been applied.

All $\frac{\partial \langle T \rangle}{\partial x}$ and $\frac{\partial \langle C \rangle}{\partial x}$ terms in the equations,

the boundary conditions in form of upwind and second order terms in equation are discretized by central difference. The successive temporary meshes are generated during the filling to evaluate the pressure and temperature profiles. Therefore, the calculations are decoupled.

TABLE 1. Properties of Resin and Fiber.

Property Material	ρ kg / m ³	C_p J / kgK	k W / (mK)	ϵ (%)	μ	L (mm)	W (mm)	Thickness (mm)
Resin	1202	2800	0.276	--	220	--	--	--
Fiber	2560	670	0.417	72	--	800	400	10

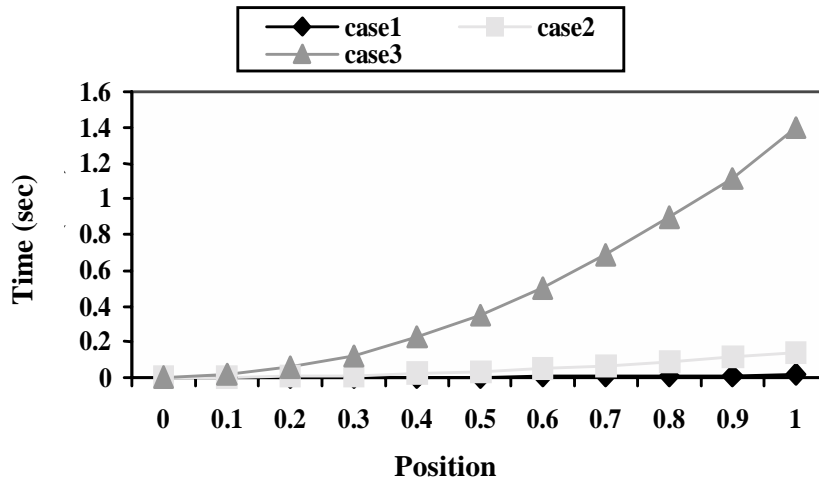
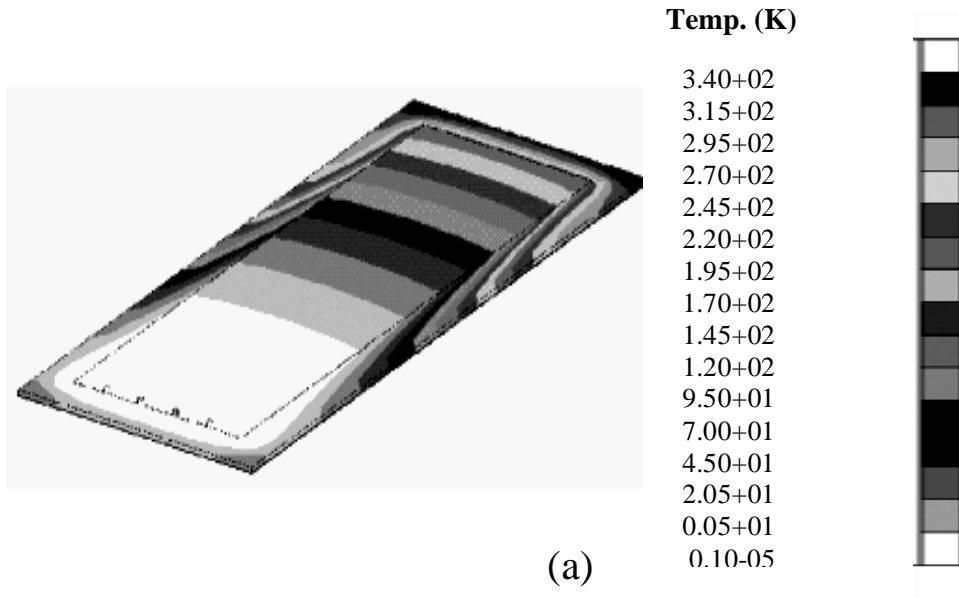
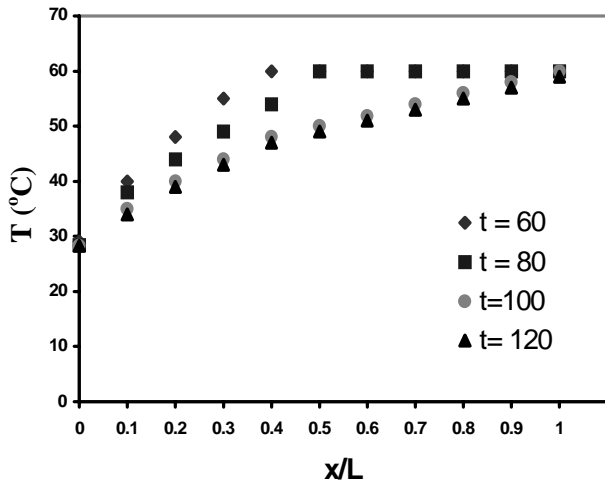
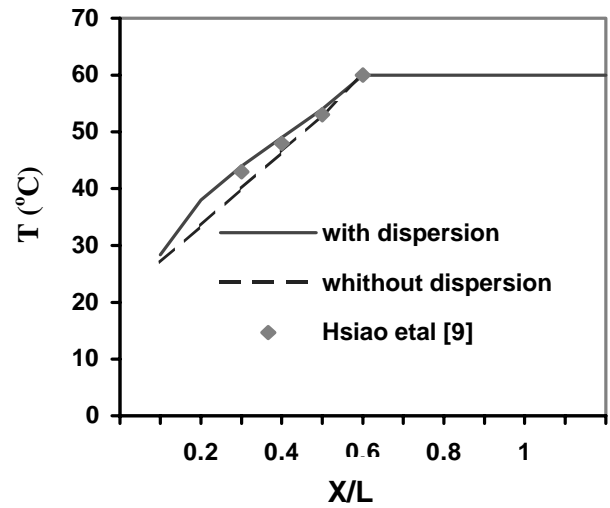


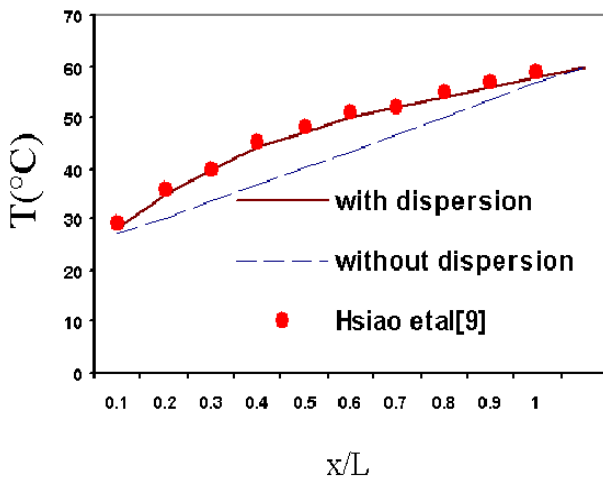
Figure 2. Flow front position at different pressure gradient: (a) sample phase profile and (b) position vs. time.



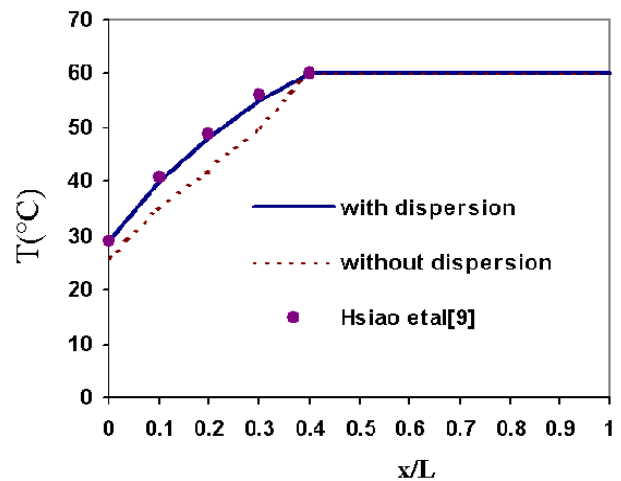
(a)



(b)



(c)



(d)

Figure 3. Temperature distribution with and without dispersion in comparison with results from Hsiao et al. [9]: (a) $t = 60$, (b) $t = 80$, $t = 100$ and (d) $t = 120$ sec.

4. NUMERICAL RESULTS

The material data used in the simulations are given in Table 1. The composite thermal conductivity is a function of the phases' conductivity through the Chang's model [8].

$$\frac{k_e}{k_f} = \frac{(2 - \epsilon_f)k_s / k_f + 1}{2 - \epsilon_f + k_s / k_f} \quad (23)$$

To model the mechanical dispersion term the conservation equations are as follows:

$$k_{dyy} = (\epsilon \rho C_p)_f b_{zz} |u|$$

$$D_{dyy} = \epsilon_f \rho_f |u| b_{zz}$$

where the typical value of the dispersion coefficient b_{zz} was selected from the literature for glass fiber mats [8].

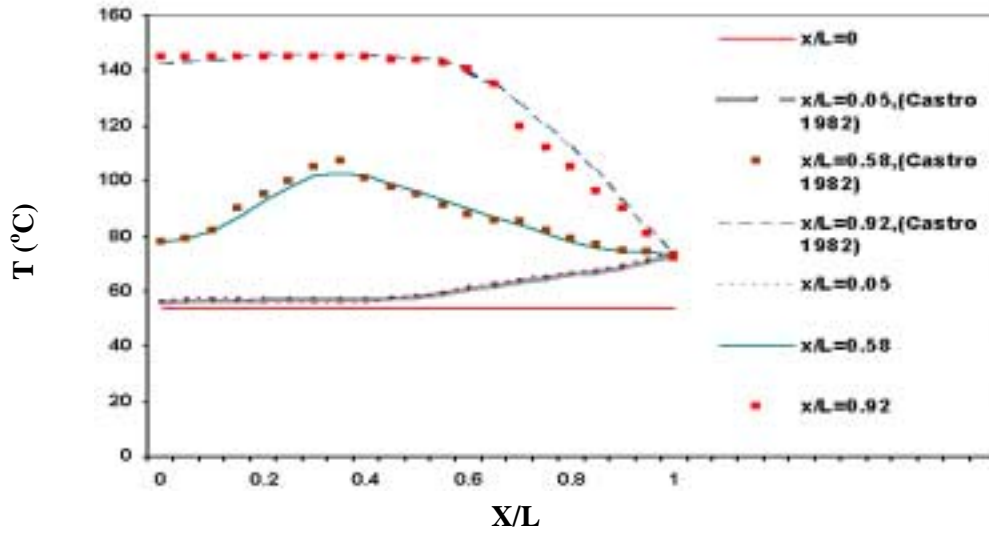
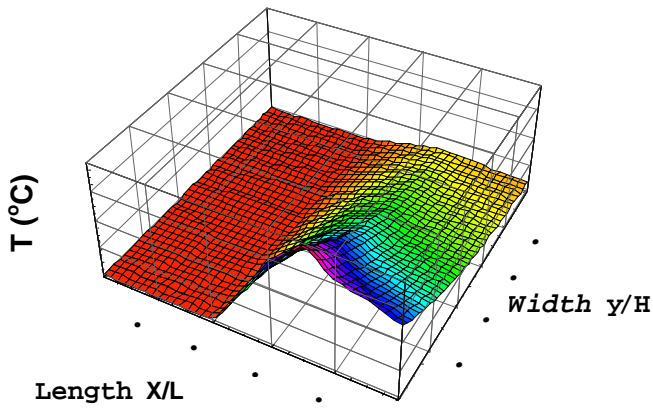
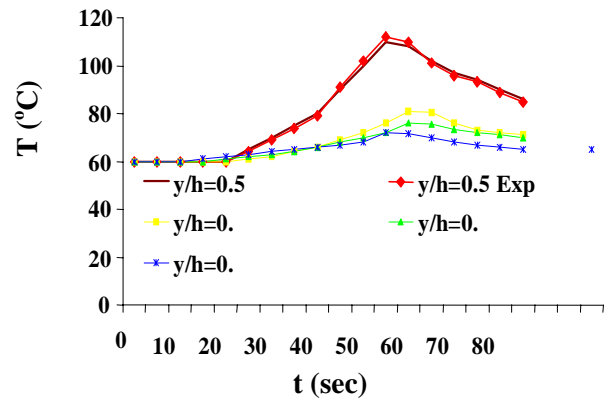


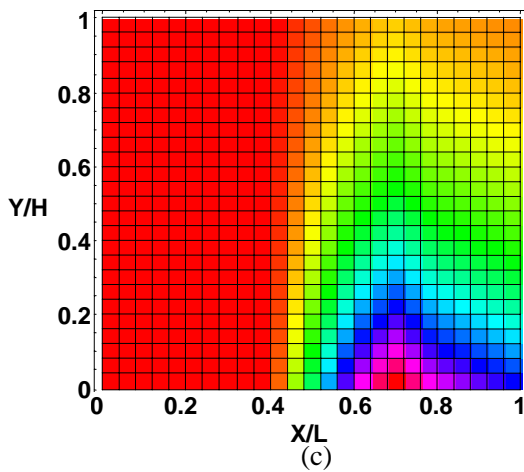
Figure 4. Temperature distribution in RTM process based on non-dimensional height in comparison with Castro et al. [7] experiments.



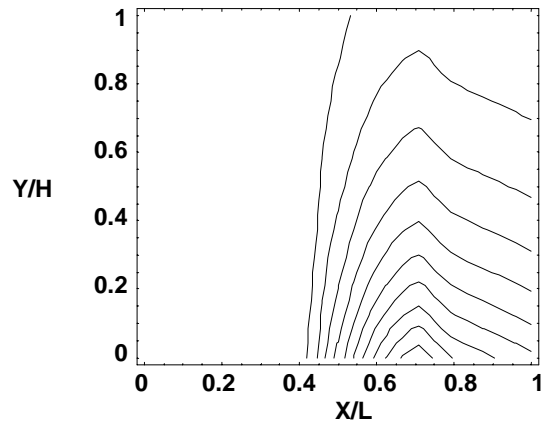
(a)



(b)

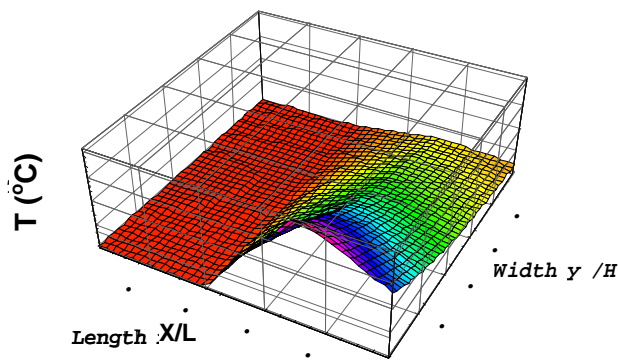


(c)

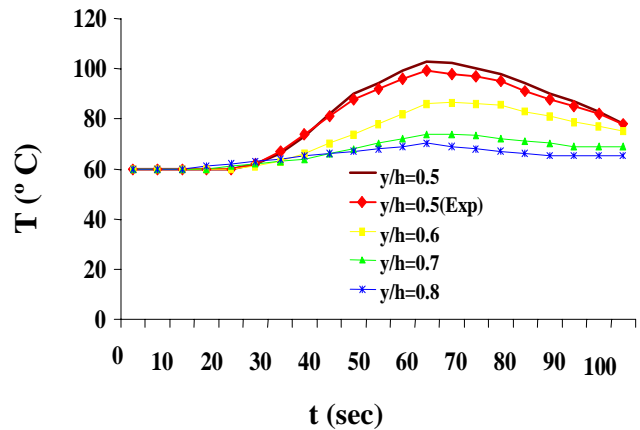


(d)

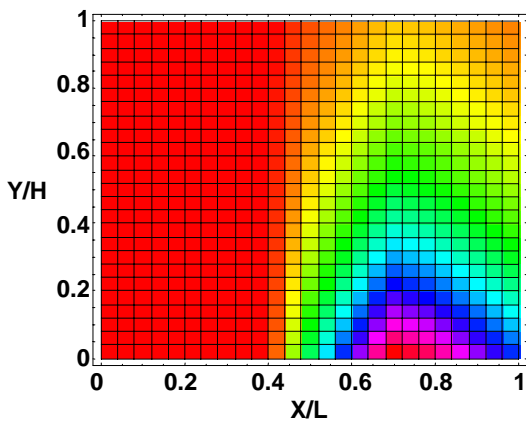
Figure 5. RTM's temperature distribution with curing reaction ($H=2$ mm).



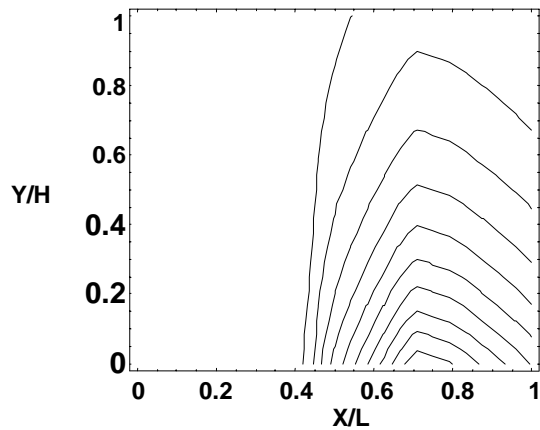
(a)



(b)



(c)



(d)

Figure 6. RTM's temperature distribution with curing reaction ($H=4$ mm).

The front flow position at the different pressure gradients has been shown in Figure 2-a. The front flow position for different gradient pressure was shown in Figure 2-b. As is seen, the process time is gradually reduced as pressure gradient increases. Also, the increase in pressure causes large difference between the measured values and the calculated ones. As was mentioned before, the effect of k_{xx} can be neglected for $Pe \ll 1$. By using this assumption and Chang's model. Figure 3 shows the temperature distribution with and without consideration of the curing. In this figure dispersion is compared with the Hsiao et al. results [9]. Figure 4 shows the temperature distribution based on y/H for different points of the mold. At the mid plane for $x/L = 0.58$, there

is a maximum temperature. The effect of curing on the temperature distribution in different positions of the medium is shown in Figure 5. Figure 5-b shows the temperature distribution for different y/h values. Also, at part (c) and part (d) of this figure the location of constant temperature was shown. This result shows that during curing, the temperature rises up to a maximum value and then decreases due to the heat conduction to the mold walls. Also, for the thicker mold, the results are shown in Figure 6. In this case, the maximum temperature value is smaller, but there is still a large temperature difference between the center and near the wall. This is the reason for the difference in properties from the center to the wall.

5. CONCLUSIONS

In this paper, a model for the non-isothermal simulation of the RTM was developed. Also, the mechanical dispersion term was included in this model. The results show the importance of mechanical dispersion and curing on the temperature field. The trial and error method was used for the exact determination of fluid free position by finite difference method. By using scale analysis, it was shown that the thermal dispersion term is negligible at the mid-surface direction in comparison with other directions. Also, the results have shown the existence of a maximum in thermal distribution during of the RTM process.

6. NOMENCLATURE

A_o	constant in the kinetic Equation 30, sec^{-1}
A_c	constant in the max conversion equation (Equation 32)
A_μ	constant in the viscosity Equation 31, Pa.s
A_v	constant in the viscosity Equation 31
\mathbf{b}	vector function for transforming the average temperature gradient into the pointwise temperature deviation
B_c	constant in the max conversion Equation 32, K^{-1}
B_v	constant in the viscosity Equation 31
c_p	specific heat, $\text{kJ/kg } ^\circ\text{C}$
C	conversion of chemical species
C_g	Max conversion
C_{hex}	$\sum_{i=s,f} (\rho c_p)_i \langle b_{xi} \rangle$
D	mass diffusivity, m^2/s
E	activation energy in kinetic Equation 30, kJ/kg
E_M	activation energy in viscosity Equation 31, kJ/kg
F_c	reaction function
h	mold half height, m
\mathbf{I}	unit tensor
k	molecular thermal diffusion, W/m K
\mathbf{K}	permeability tensor, m^2
\mathbf{n}	Unit outward normal vector
P	Pressure, bar
t	Time, sec

T	Temperature, $^\circ\text{C}$
T_{inflow}	Input temperature of fluid, $^\circ\text{C}$
u	Velocity component, m/s
\mathbf{V}	Velocity vector, m/s
x,y,z	Co-ordinates
ε	Volume fraction
μ	Resin viscosity, Pa. s
ρ	Density, kg/m^3
ΔH	Heat of reaction, kJ/kg
$\langle \rangle$	Volume average
$\langle \rangle^f, \langle \rangle^s$	Intrinsic phase averages over the fluid and solid phase

Subscripts

f	Fluid (resin)
s	Solid (fiber)
i	Solid and fluid
w	Wall
e	Effective
D	Dispersion
c	Characteristic
Inflow	At inlet

7. REFERENCES

1. Bruscke, M. V. and Advani, S. G., "A Numerical Approach to Model, Non-Isothermal, Viscous Flow with Free Surface Through Fibrous Media", *Int. J. Numer. Methods Fluids.*, 19, (1994), 575-603.
2. Liu, B. and Advani, S. G., "Operator Splitting Scheme for 3-D Flow Approximation", *Computational Mechanics J.*, 38, (1995), 74-82.
3. Tucker, C. L. and Dessenberger, R. B., "Chap 8: Governing Equations for Flow and Heat Transfer in Stationary Fiber Beds", In flow and Rheology in Polymer Composites Manufacturing, Edited by S. G. Advani, Elsevier, Amsterdam, (1994).
4. Dessenberger, R. D. and Tucker, C. L., "Thermal Dispersion in Resin Transfer Molding", *Polymer Composites*, 16(6), (1995), 495-506.
5. Mal, O., Couniut, A. and Depert, F., "Non-Isothermal Simulation of the Resin Transfer Molding Process", *Composites Part A*, 29, (1998), 180-198.
6. Mal, O., "Modeling and Numerical Simulation of Reaction Injection Molding Processes", PhD thesis, (1999).
7. Castro, J. and Macosko, C., "Studies of Mold Filling and Curing in the Reaction Injection Molding Process", *AIChE J.*, 28, (2000), 250.
8. Kaviany, M., "Principle of Heat Transfer in Porous Media", Springer-Verlag, New York, (1991).

9. Hsiao, K. T., Loudorn, H. and Advani, S. G.,
“Experimental Investigation of Heat Dispersion due
to Impregnation of Viscous Fluids in Heated During

Fibrous Porous Composites Processing”, *Journal
of Heat Transfer*, Vol. 123, (February 2001), 178-
186.